Deformation Field Estimation for the Cardiac Wall using Doppler Tissue Imaging.

Valérie Moreau[1], Laurent D. Cohen[1], and Denis Pellerin[2]

[1] CEREMADE, University of Paris-Dauphine, 75775 Paris cedex 16, France,
{moreau,cohen}@ceremade.dauphine.fr
[2] St George's Hospital Medical School,University of London.

Abstract. This paper presents different ways to use the Doppler Tissue Imaging (DTI) in order to determine deformation of the cardiac wall. As an extra information added to the ultrasound images, the DTI gives the velocity in the direction of the sensor. We first show a way to track points along the cardiac wall in a M-Mode image (1D+t). This is based on energy minimization similar to a deformable grid. We then extend the ideas to finding the deformation field in a sequence of 2D images (2D+t). This is based on energy minimization including spatio-temporal regularization and a priori constraints.

Keywords: Cardiac image processing, Ultrasound Image, Doppler Tissue Imaging, motion estimation, multi-modality image fusion.

1 Introduction

Doppler Tissue Imaging (DTI) is a recent technique which provides a partial information about the myocardial wall velocities. This is the velocity of the tissues in the direction of the sensor. This new data is represented by a colour added to the conventional ultrasound image. Two types of these images are used by the cardiologists. First 2D images as in figure 1.a. are usually employed in ultrasound imaging. But the extra data which is collected during the acquisition implies a reduction of the temporal resolution compared to classical ultrasound. We cannot have more than a hundred images per second. M-Mode images (Figure 1.b) can give a better temporal resolution by reducing the studied area. They are obtained by choosing a 1D segment on the image and watching its evolution through time. Since there is only one dimension the temporal resolution is increased to about 500 frames per second. In this work, we used sequences of images of left ventricle of human hearts.

Previously, M-mode images have been studied in [1] in order to track the cardiac wall with a variant of active contours. The contour $C(t) = (t, f(t))$ deforms to minimize $E(f) = \int_0^T \omega_1 |f'(t)|^2 + \omega_2 |f''(t)|^2 + P_{edge}(C(t)) + P_{velocity}(C(t))dt$. P_{edge} and $P_{velocity}$ are potentials which attract respectively $C(t)$ to the edge and $f'(t)$ close to the velocity measured by the DTI. [1] shows the advantage of using DTI in addition to the edge information.

We will use different variational methods to study the deformation of the heart in M-mode and afterwards 2D DTI images.

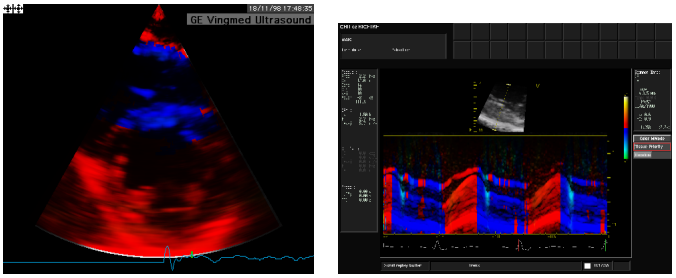

(a) 2D Ultrasound Image.

(b) M-Mode Ultrasound Image.

Fig. 1. DTI Images.

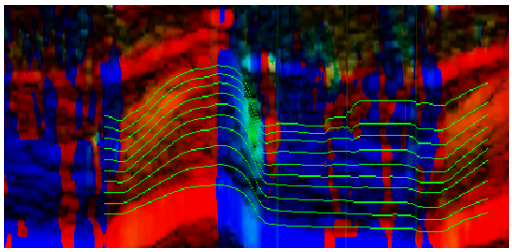

Fig. 2. Initialization of the steepest gradient descent.

2 Tracking the Wall through M-Mode Images

We now want to track several points through the cardiac wall on the M-Mode image $I(t,z)$, making use of the velocity given by the DTI image $v_{DTI}(t,z)$. Points are chosen for the initial time $t=0$ along a hand given segment. They are regularly spaced on this vertical segment as seen on the left of figure 2.

Let $\{C_i(t) = (t, y_i(t))\}_{1\leq i\leq N}$ be the curves which perform the tracking of these points. If the points we want to follow are close enough, the curves $\{C_1,\dots,C_N\}$ must be consistent with one another. In order to improve the tracking, we will consider the set of curves $\{C_1,\dots,C_N\}$ as an active net: $(y(t,s)=y_s(t))_{s,t}$ where only the second coordinate $y(t,s)$ can vary. The active nets, or deformable grids, are defined in [2] and [3]. The net deforms according to the minimization of an energy. Our energy consists of three terms.

1. A regularization term as in [2].
   $E_{reg}(y) = \iint \alpha(\frac{\partial y}{\partial s}^2 + \frac{\partial y}{\partial t}^2) + \beta(\frac{\partial^2 y}{\partial s^2}^2 + 2\frac{\partial^2 y}{\partial st}^2 + \frac{\partial^2 y}{\partial t^2}^2)dtds$
   This term will be the one enabling interaction between successive curves. The first derivatives make the net contracts (which should be avoided by choosing α small) and the second derivatives enforce smoothness and rigidity.

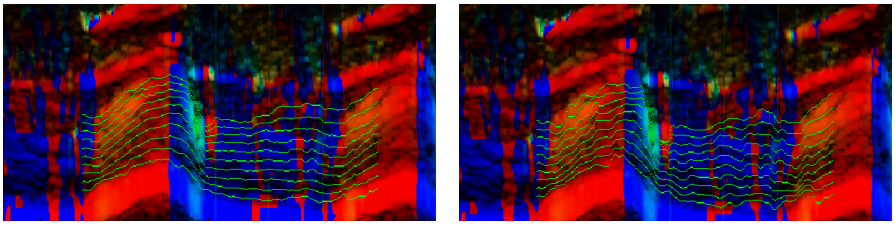

(a) After a few iterations of steepest gradient descent.

(b) Result of the tracking.

Fig. 3. Steepest gradient descent.

2. An external term which attracts the derivative close to the given velocity measured by the DTI. This is an extension in two dimensions of [1].
   $E_{velocity}(y) = \iint (\frac{\partial y}{\partial t} - v_{DTI}(t, y(t,s))^2 dtds$
3. The last term is also an external term. We assume that the gray level is nearly constant along and around each curve.
   $E_{gray}(y) = \iint \sum_{k=-2}^{k=2} (I(t, y(t,s)+k) - I(0, y(0,s)+k)^2 dsdt$

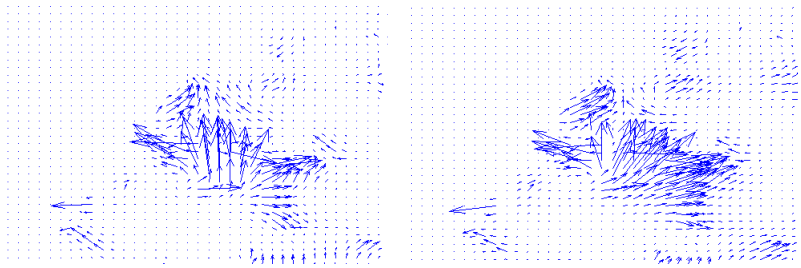

(a) Optical Flow. Close up. Bottom of the lateral wall.

(b) Velocity field obtained by our method on the same case.

Fig. 4. Comparison between optical flow and the velocity field we obtained. In these images, the sensor is above and on the right of the pictures.

We used both DTI and gray scale conventional ultrasound in this energy. The net y is obtained by the minimization of $E(y) = E_{reg}(y) + \mu E_{gray}(y) + \lambda E_{velocity}(y)$ where λ and μ are postive constants. μ must be chosen small because E_{gray} is very sensitive to noise. We proceed as in [1] and [4] and use a steepest gradient descent, the discretization was done by finite differences. This gives in matrix form $(Id + \tau A)Y^{n+1} = Y^n + \tau F(Y^n)$ where Y is the discrete version of y and A is a sparse square matrix. To avoid a large matrix inversion, we can approximate $(Id+\tau A)^{-1} \approx Id - \tau A$ for τ small enough. We then apply a SOR algorithm [5]. The energy can have many local minima. Therefore we must

use an initialization close to the solution. For this purpose, we choose an integration of the velocity measured by the DTI: $y(t+1,s) \approx y(t,s) + v_{DTI}(t, y(t,s))dt$ (figure 2) where dt is the time step. These curves, which are the direct interpretation of the DTI velocity do not provide an accurate tracking of the wall. We can see that some curves leave the wall during the tracking. The hypothesis about the gray level is not exact in the case of ultrasound images. Nevertheless figure 3 shows how this term of the energy tends to correct the tracking processed using only DTI. Figure 3.b presents a final result. We have compared these curves to manually traced curves by the cardiologist. We notice that the set of curves folow precisely the deformation of the cardiac wall. This automatic tracking has been of much help for cardiolgists in order to study various use of DTI images [6], [7].

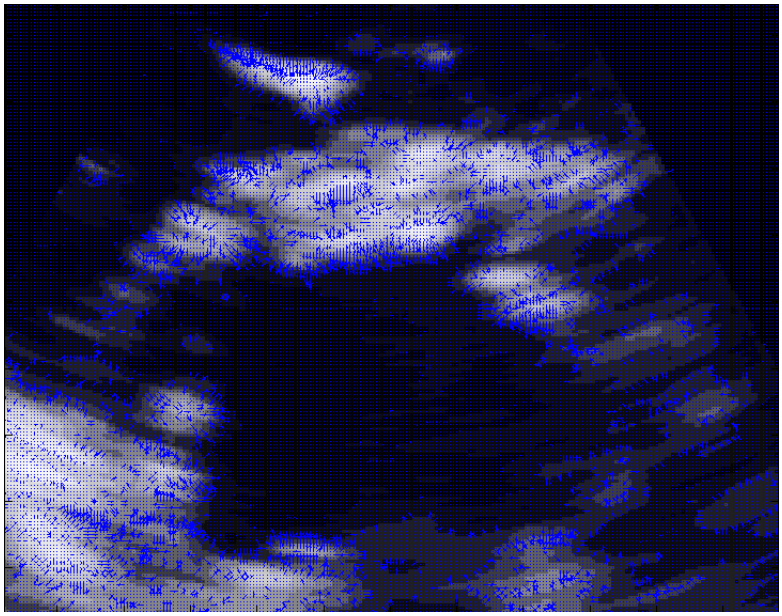

Fig. 5. Velocity field with the simplest method.

3 Deformation Field in a 2D Image Sequence

3.1 Presentation

Our next interest is the study of 2D image sequences. The difficulties raised are the low temporal resolution and the incomplete DTI information. The DTI only measures the velocity in the direction of the sensor. Moreover the acquisition of the sequence instead of a single image implies a lower spatial resolution. Our motivation is to be able to diagnose a pathology with the help of DTI ultrasound images. For that purpose, we are mostly interested in recovering a complete deformation field.

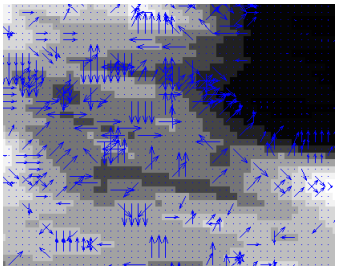

Fig. 6. Close up on figure 5.

3.2 Recovering the Velocity Field

The DTI sequence contains two types of information: the velocity $v_{DTI}(x, y, t)$ in the direction of the sensor measured by the DTI and the conventional ultrasound sequence $I(x, y, t)$. We will use this second information to complete the first one. From the grayscale conventional ultrasound sequence, we can calculate the optical flow [8], [11], [9] and [10]. The optical flow is the distribution of apparent velocity of motion of brightness patterns in an image. The determination of the optical flow is based on the hypothesis that the brightness of a point $I(x(t), y(t), t)$ is constant through time. Using the chain rule for differentiation we see that $\frac{\partial I}{\partial x}\frac{\partial x}{\partial t} + \frac{\partial I}{\partial y}\frac{\partial y}{\partial t} + \frac{\partial I}{\partial t} = 0$. If we let $u = \frac{\partial x}{\partial t}$ and $v = \frac{\partial y}{\partial t}$, we have a linear equation in the two unknows u and v : $I_x u + I_y v + I_t = 0$, where $I_x = \frac{\partial I}{\partial x}$, $I_y = \frac{\partial I}{\partial y}$ and $I_t = \frac{\partial I}{\partial t}$. This is called the constraint of the optical flow. It does not define a unique solution. Our solution is inspired by the Horn and Schunck's method and will take advantage of the knowledge of the DTI information. The field we are looking for will satisfy three constraints:

1. The optical flow constraint.
2. The agreement with the DTI velocity.
3. A regularity constraint.

These properties are obtained as follows: we look for a vector field (u, v) which minimizes

$$E(u,v) = \iint_{\Omega} (x_{DTI}u + y_{DTI}v - v_{DTI})^2 + \alpha(\|\nabla u\|^2 + \|\nabla v\|^2) + \beta(I_x u + I_y v + I_t)^2 dxdy$$

where α and β are positive constants, Ω is the image domain, (x_{DTI}, y_{DTI}) denotes the direction of the sensor and v_{DTI} denotes the norm of the velocity measured by the DTI. We minimize this energy with a steepest gradient descent. We used a discretization by finite differences with an explicite scheme. We give an example in the figure 5. All the examples were obtained on the same image taken during the systole. The results are satisfying compared with simple optical flow (figure 4). We get a more regular field without increasing the diffusion. We observe that the velocity field mainly represents a motion of contraction. But this field is still very noisy.

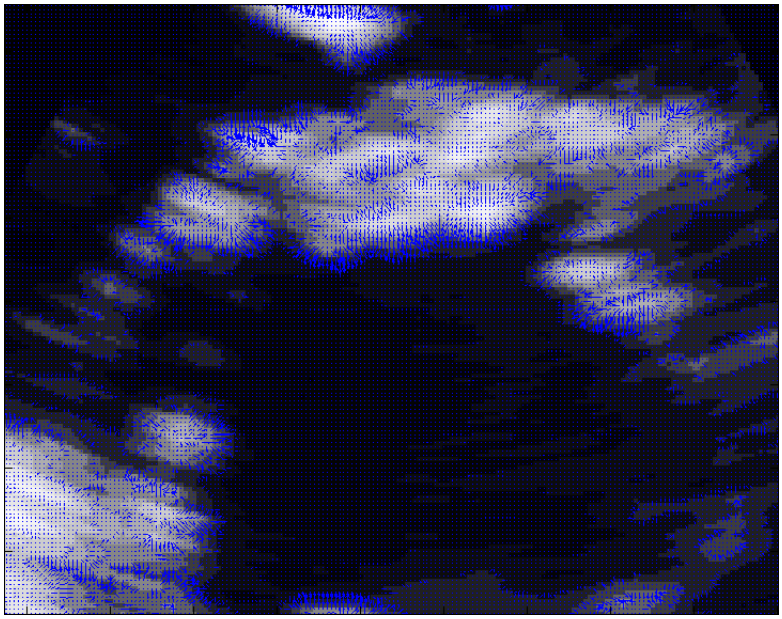

Fig. 7. Velocity field with a spatio-temporal regularization.

We can improve the results by using the idea of [11]. It consists of using a spatio-temporal regularization instead of a spatial regularization. It leads us to process the whole sequence simultaneously by minimizing the following energy:

$$E(u,v) = \iiint_{\Omega\times[0;T]} (x_{DTI}u + y_{DTI}v - v_{DTI})^2 + \alpha(\|\nabla u\|^2 + \|\nabla v\|^2) \\ +\beta(I_x u + I_y v + I_t)^2 dxdydt.$$

The rest of the algorithm is the same. An example of result is shown if figure 7. As in [11], the result is much more coherent and complete.

In order to improve results, we set soft constraints from a priori information about the heart deformation. In this type of image, the deformation is a contraction. Its center is the center of the heart. We then imposed a radiality constraint on the energy. Let $O = (x_O, y_O)$ be the center and radiuses R_1 and R_2 define a ring around the myocardium wall: $C(O, R_1, R_2) = \{(x,y), R_1 \leq d(O,(x,y)) \leq R_2\}$. We add a term to the energy of the form $\int_{[0;T]}\iint_{C(O,R_1,R_2)}(u.(x-x_o) - v.(y-y_o))^2 dxdydt$. We obtain figure 9. We can see the result of the constraint on the direction of the field but we could lose information while giving too much a priori information. The choice of adding this constraint or not is dependent on the application.

We checked the validity of our results by deforming an image with the velocity field and comparing to the following image, both visually and with a quadratic

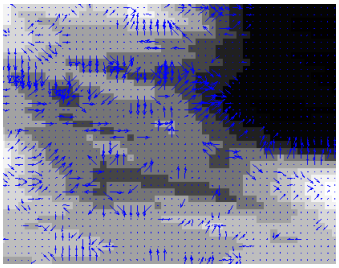

Fig. 8. Close up on figure 7.

norm. This comparison gave good results, but, since we calculate a smooth field, it is not an quantitative evaluation of the quality of the velocity field. In future work, we will analyse the deformation field by the way of segmentation and classification algorithms. Then we will compare these analysis with other medical datas. That is how we will be able to check this deformation field estimation.

4 Conclusion

We have presented different ways to use the Doppler Tissue Imaging (DTI) in order to determine deformation of the cardiac wall. We first showed a way to track points along the cardiac wall in a M-Mode image (1D+t), based on a deformable grid energy minimization. We then showed how to estimate the deformation field in a sequence of 2D images (2D+t), based on energy minimization including spatio-temporal regularization and a priori constraints. Future work includes analyzing the deformation of the cardiac wall and finding pathology starting from the deformation field method we described in this paper.

References

1. L. D. Cohen, F. Pajany, D. Pellerin, and C. Veyrat. Cardiac wall tracking using doppler tissue imaging (DTI). In *In Proc. of International Conference on Image Processing (ICIP'96)*, pages III–295–298, Lausanne, Switzerland, Sept. 1996.
2. M. Bro-Nielsen. Active Nets and Cubes. *Technical Report, Institute of Mathematical Modelling, Technical University of Denmark*, Nov 1994.
3. K. Yoshino, T. Kawashima and Y. Aoki. Dynamic Reconfiguration of Active Net Structure. *Asian Conference on Computer Vision*, November 1993.
4. L.D. Cohen. On active contours models and balloons. *Computer Vision, Graphics, and Image Processing: Image Understanding*, 53(2):211-218 March 1991.
5. A. Blake, A. Zisserman, *Visual Reconstruction.* MIT Press, 1987.
6. C. Veyrat, D. Pellerin, L.D. Cohen,F. Larrazet, F. Extramiana, and S. Witchitz Spectral, one-or two-dimensional tissue velocity doppler imaging: which to choose? *Cardiology*, 9(1):9–18, 2000.
7. D. Pellerin, A. Berdeaux,L.D. Cohen,J.F. Giudicelli,S. Witchitz, and C. Veyrat, Comparison of two myocardial velocity gradient assessment methods during dobutamine infusion using doppler myocardial imaging. *Journal of the American Society of Echocardiography*, 12:22–31, 1999.
8. B.K.P. Horn and B.G. Schunck. Determining Optical Flow. *Artificial Intelligence*, (17) (1-3) :185–204, 1981.
9. G. Aubert, R. Deriche and P. Kornprobst. Optical flow estimation while preserving its dicontinuities: A variational approach. *Proceedings of the second asian conference on computer vision.*,1995

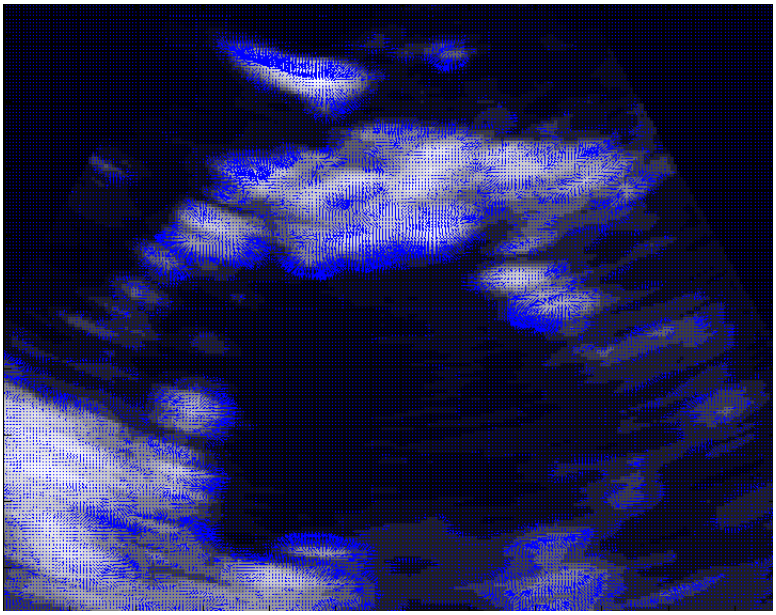

Fig. 9. Velocity field with a radiality constraint.

10. J.L. Barron, D.J. Fleet, S.S. Beauchemin, Performances of optical flow techniques. *International Journal of Computer Vision*, 12(1) p.43-77 (1994).
11. J. Weickert et C. Schnorr. Variational Optic Flow Computation with a Spatio-Temporal Smoothness Constraint. *Journal of Mathematical Imaging and Vision*, 14(3), May 2001.

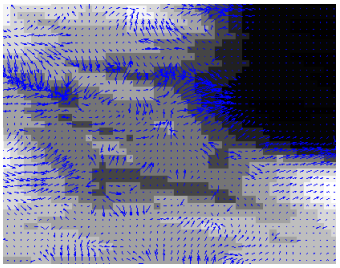

Fig. 10. Close up on figure 9.